Asian Journal of Chemistry; Vol. 30, No. 9 (2018), 2069-2074

ASIAN JOURNAL OF CHEMISTRY

https://doi.org/10.14233/ajchem.2018.21427

Zinc Oxide Nanoparticles Dispersed *p*-(*p'*-Ethoxy benzylidene)-*p*-cyano aniline Mesogen: Statistical and Spectral Analysis

K.V. Surya Narayana Raju[1], Shaik Babu[1] and Shaik Salma Begum[2,*]

[1]Department of Physics, Koneru Laxmaiah Educational Foundation, Vaddeswaram-522 502, India
[2]Department of Physics, NRI Institute of Technology, Pothavarappadu-521 212, India

*Corresponding author: E-mail: dr.ssbmj@gmail.com

Received: 7 May 2018; *Accepted*: 9 June 2018; *Published online*: 31 July 2018; AJC-19022

Bathochromic shift in terms of temperature was noticed in *p*-(*p'*-ethoxy benzylidene)-*p*-cyano aniline (EBCA) on dispersion of nano ZnO particles and all the computed optical properties like birefringence, absorption coefficient, phase retardation, order parameter, *etc*. through statistical method of textures exhibit hypsochromic shift in their values. These changes were assigned to perturbation of lattice arrangement of host EBCA mesogen due to nano ZnO particles. The present studies also confirm the controversial behaviour of material when brought to nano size. Techniques involved in the current investigation are polarizing optical microscopy, differential scanning caloriemetry, powder X-ray diffraction spectroscopy and statistical analysis using MatLab. Detailed analyses of observed changes in nano dispersed *p*-(*p'*-ethoxy benzylidene)-*p*-cyano aniline (EBCA) were reported.

Keywords: ZnO nanoparticles, *p*-(*p'*-Ethoxy benzylidene)-*p*-cyano aniline, Birefringence, Order parameter.

INTRODUCTION

Birefringence and order parameter are key points to judge the applications of liquid crystals (LC) in various fields of science and technology. Various methods are proposed to compute these parameters for liquids and liquid crystals [1-5]. Most common method of calculating birefringence is from the measurement of refractive indices [6-10]. However, recent investigations revealed that the birefringence can be calculated simply by using mathematical methods through image analysis of liquid crystal samples [11-15]. Present study also involved calculations of various optical parameters like absorption coefficient, birefringence, order parameter, *etc*. through statistical methods of textural images. Here, a comparative study was taken to pure and nanoparticles dispersed mesogens. Till now various analyses were done to almost all the pure mesogens [16-21], which found little drawbacks in application point of view [22-24]. However, addition of foreign elements to the lattice of pure mesogen perturbs transition temperatures optical parameters and various thermodynamical parameters, because mesogen is a soft and sensitive matter. Research has been going on in this way and found remarkable variations in the impure mesogens [25-30].

Also, dispersion of nanoparticles especially metal oxide nanoparticles to pure liquid crystal were studied in various laboratories which found noticeable applications in terms of power consumption [31-34]. Present work was also done in the same way by considering zinc oxide nano particles and introducing them in the lattice of *p*-(*p'*-ethoxy benzylidene)-*p*-cyanoaniline (EBCA) which is pure nematic liquid crystal. Remarkable changes were found in thermodyn-amical and optical parameters and these helped to predict that zinc oxide nanoparticles dispersed *p*-(*p'*-ethoxy benzylidene)-*p*-cyanoaniline (EBCA) found applications in high temperature fields.

EXPERIMENTAL

The used liquid crystals of *p*-(*p'*-ethoxy benzylidene)-*p*-cyanoaniline (EBCA, **1**) is the product of Frinton Laboratory, USA. All the reagents zinc nitrate [$Zn(NO_3)_2 \cdot 6H_2O$] and NaOH used for preparation of ZnO nanoparticls were collected from Merck Chemical Industrial company and used without any further purification.The alkali solution of zinc was prepared by dissolving in distilled water to form a 100 mL solution [Zn^{2+} = 0.5 M, OH = 1.0 M].

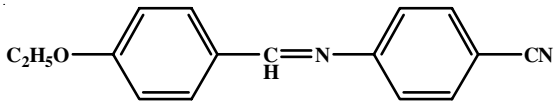

Molecular structure of liquid crystal *p*-(*p*′-ethoxy benzylidene)-*p*-cyanoaniline (EBCA, **1**)

Preparation of ZnO nanoparticles: Zinc oxide nanoparticles were prepared by following procedure. Zinc nitrate and NaOH used for preparation of ZnO nanoparticles. To form 0.5 M solution 100 mL pure water added to $Zn(NO_3)_2 \cdot 6H_2O$. The solution was heated to 60 ºC while stirring for 2 h at same temperature. After few hours, white precipitate was collected and washed with distilled water. The obtained solution was maintained at pH 10 by adding NaOH solution and left for over night at room temperature. The precipitate was centrifuged and dried at room temperature, white ZnO particles obtained [12].

Preparation of nanoparticles doped liquid crystal (nEBCA): The ZnO nanoparticles and *p*-(*p*′-ethoxy benzylidene-*p*-cyanoaniline (EBCA) in the proportion of 100:1 were mixed. Then the liquid crystals were mixed by melting them together in a fusion tube to obtain homogeneous mixture. The mixture then cooled down to obtain solid which was grounded. The nanoparticles are doped into liquid crystals mixture in the concentration of 0.1% wt. After that liquid crystal prepared mixtures (nEBCA) were introduced to the sandwich cell by capillary action at 40 ºC.

Procedure: The available glass slide was cleaned with acetone and rubbed such order to make unidirectional alignment. A small amount of liquid crystal was placed on the glass slide. A small cover slip was placed on the sample. The glass slide is mounted on a hot stage of the microscope to record the textural changes in the sample. Meopta polarizing optical microscope (POM) connected with hot stage and camera attachment is used to record the textures of the sample [35]. Sample textures were recorded at cooling rate @2 ºC/min in three monochromatic image planes of red, green, and blue at wavelength 600, 530 and 470 nm, respectively, under crossed and parallel polarizer [36]. The image textures detected by camera and the intensity values of pixels ranges from 0 to 255. The dimensions of image were selected to be 256 × 256. MATLAB software was used to computational analysis of textures of the samples such as mean, variance, skewness, kurtosis, absorption coefficient, birefringence, order parameter, phase retardation [37]. The structural and optical properties of the prepared nEBCA particles have been confirmed using TEM and XRD.

RESULTS AND DISCUSSION

The TEM image of used ZnO nanoparticles for preparing the nano doped liquid crystal is shown in Fig. 1. The rod shape of ZnO nanoparticle confirmed by TEM image analysis, which makes it suitable for doping in rod shaped nematic liquid crystal matrix. The ZnO nanoparticle average size is 34 nm determined by using Scherrer formula [38].

Now a days, the technique of image analysis is very useful to investigate the physical properties and compute the statistical parameters as a function of temperatures for liquid crystals. The polarizing optical microscope is used to capture the textures

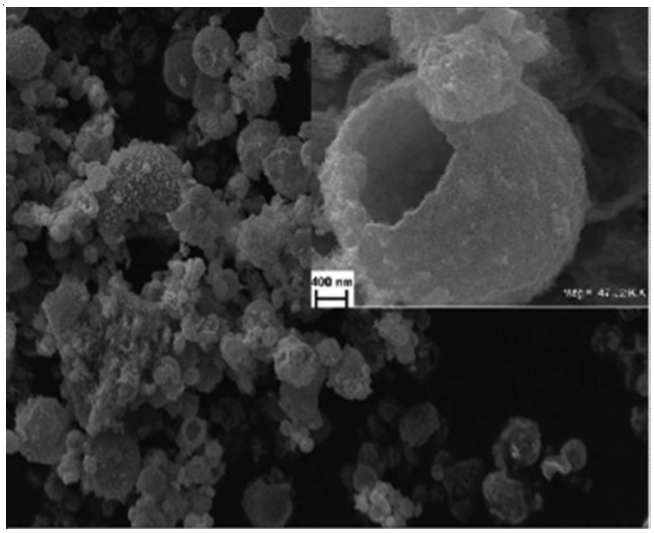

Fig. 1. TEM images of ZnO (1 % Cu doped) nanoparticles

of liquid crystals in the studies of thermo optical properties of EBCA and nEBCA. At present glance, the textures closely resembles textures commonly observed for nematic liquid crystals. The nematic phase of EBCA temperature range is 112.5 ºC and the temperature range of mixture of ZnO in EBCA is 134 ºC.

The liquid crystalline compound *p*-(*p*′-ethoxy benzylidene)-*p*-cyanoaniline with dispersed ZnO nanoparticles done an observable change occurred when the liquid crystalline compounds dispersion with nanoparticles . Liquid crystalline phases are not disturbed with the dispersion of nanoparticles whereas more advantageous in various applications. The transition temperatures and textures are obtained by using polarizing microscope (POM) and along with transition temperatures, enthalpy values are obtained from differential scanning calorimetry (DSC). Transition temperatures of EBCA and ZnO dispersed EBCA are given in Table-1.

TABLE-1
TRANSITION TEMPERATURES OF EBCA AND ZnO NANOPARTICLES DISPERSED EBCA (nEBCA)

Sample	TS-N	TN-I
EBCA (POM)	74.0 °C	112.50 °C
EBCA (DSC)	76.6 °C	116.30 °C
EBCA (image analysis)	80.1 °C	113.05 °C
NEBCA (POM)	103.0 °C	130.00 °C
NEBCA (DSC)	105.3 °C	123.50 °C
NEBCA (image analysis)	104.9 °C	129.70 °C

It is observed that the textual images were same due to the self-assembly of ZnO nanoparticles but thermal range of nematic phase is slightly changed by the dispersion of nanoparticles. The change in enthalpy at the phase transformations and transition temperatures determined by POM and DSC techniques. The transition temperatures are increased with ZnO nanoparticles dispersed in EBCA when compared to its pure counterpart. Textures of EBCA and nEBCA are shown in Fig. 2 and 3, while the textures of nematic phases of EBCA and nEBCA are shown in Fig. 4 and 5, respectively.

The differential scanning calorimetry of EBCA and nanoparticles dispersed EBCA (nEBCA) liquid crystals were taken in the temperature range of 20-200 ºC@2 ºC/min. The

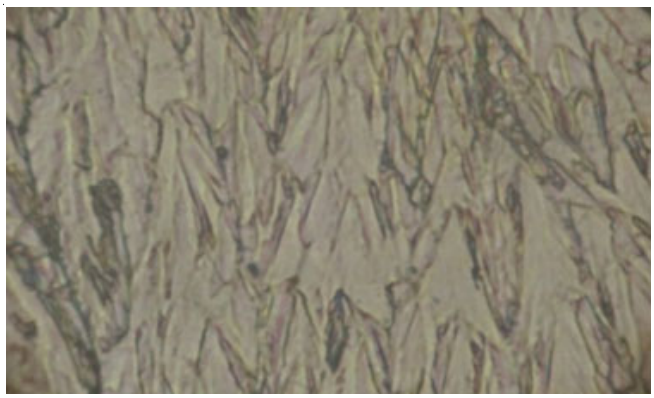

Fig. 2. Texture of EBCA at 30 °C

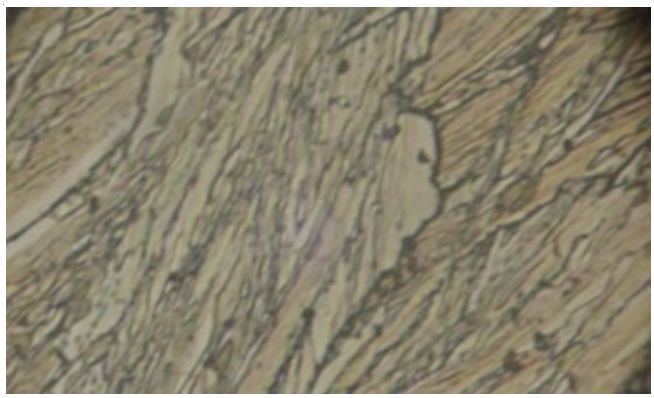

Fig. 3. Texture of nEBCA at 30 °C

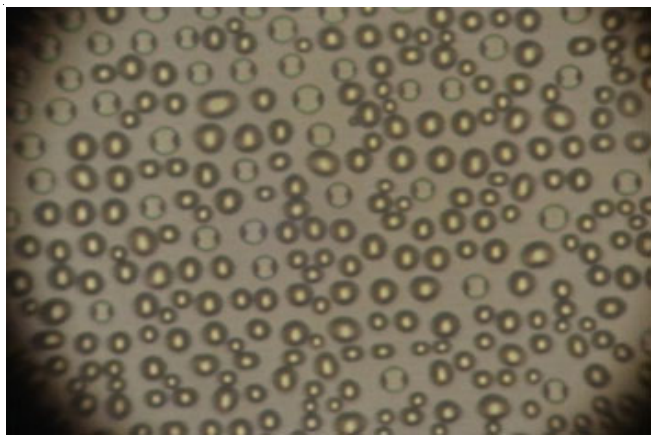

Fig. 4. Nematic phase of EBCA at 75 °C

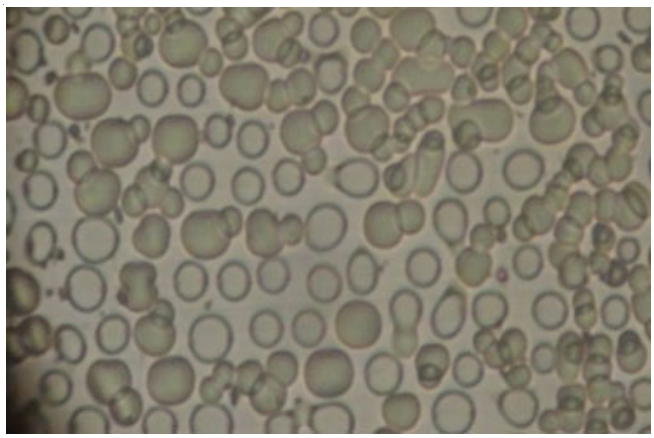

Fig. 5. Nematic phase of nEBCA at 115 °C

thermograms are displayed in Figs. 6 and 7. It is clear that nanoparticles influence on the host lattice (EBCA) of liquid crystal. The nanoparticles dispersed EBCA (nEBCA) shows enhanced transition temperatures both in crystal-nematic ($T_{C\text{-}N}$) and nematic-isotropic ($T_{N\text{-}I}$) phase changes over that of pure EBCA liquid crystal. These predominant changes in the thermal properties of the host material are attributed to the high melting temperature of zinc oxide nanoparticles that were dispersed. This helps to suggest the material of nEBCA in high temperature applications of liquid crystals.

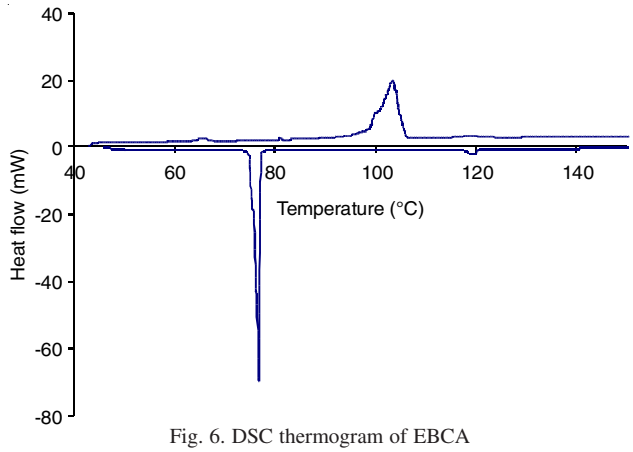

Fig. 6. DSC thermogram of EBCA

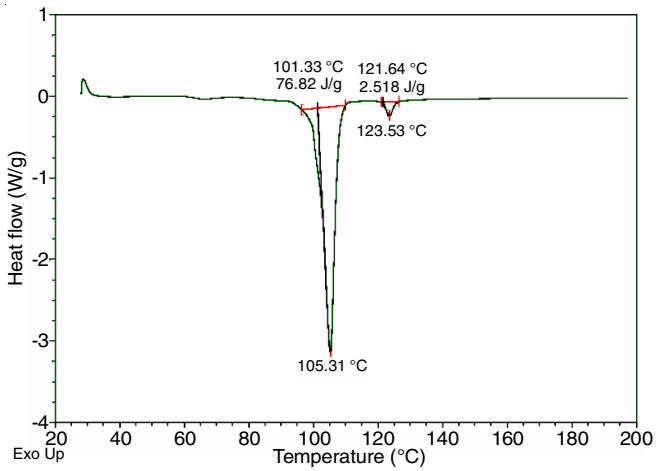

Fig. 7. DSC thermogram of nEBCA

The defined statistical parameters *viz*., mean, varience, skewness, kurtosis, absorption coefficient, birefriengnce, order parameter and phase retardation are computed from the textures of samples observed by POM at different temperatures. The experiments were done at both heating and cooling and in all cases the plots are drawn for heating cycles similar behaviour observed for cooling cycles. The abrupt changes in the statistical parameter indicate the consequent changes in the features of the textures of samples with respect to temperature due to the phase transition of material. Mean value of nEBCA increases, and varience skewness and kurtosis decreases. The phase reatardation of nEBCA was also increased and finally absorption coefficient birefringence and order parameter values were significantly decreased with increased temperature. When comparing the order parameter value for nEBCA compounds with the pure mesogen, the present parameter shows low value.

The statistical parameters computed from the translated version of colour mode for optical texture of EBCA compound at 108 ºC and for nEBCA at 118 ºC are tabulated in Table-2. The optical parameters for the same are also tabulated in Table-3.

Figs. 8a and 8c indicate mean and variance, skewness and kurtosis for EBCA a significant peak was observed at 110 ºC, while Figs. 8b and 8d indicates that for nEBCA, three significant peaks were observed at the temperatures between 118 ºC to 134 ºC. In Fig. 8e, a significant dip in absorption coefficient of EBCA was found at 108 ºC and finally decreases at isotropic phase, whereas for nEBCA a significant dip is at around 110

TABLE-2
STATISTICAL PARAMETERS FOR EBCA & nEBCA

Compound	EBCA	nEBCA
Mean	133.5	134
Variance	55	55
Skewness	1	-4.5
Kurtosis	3	6
Absorption coefficient	5000	5000

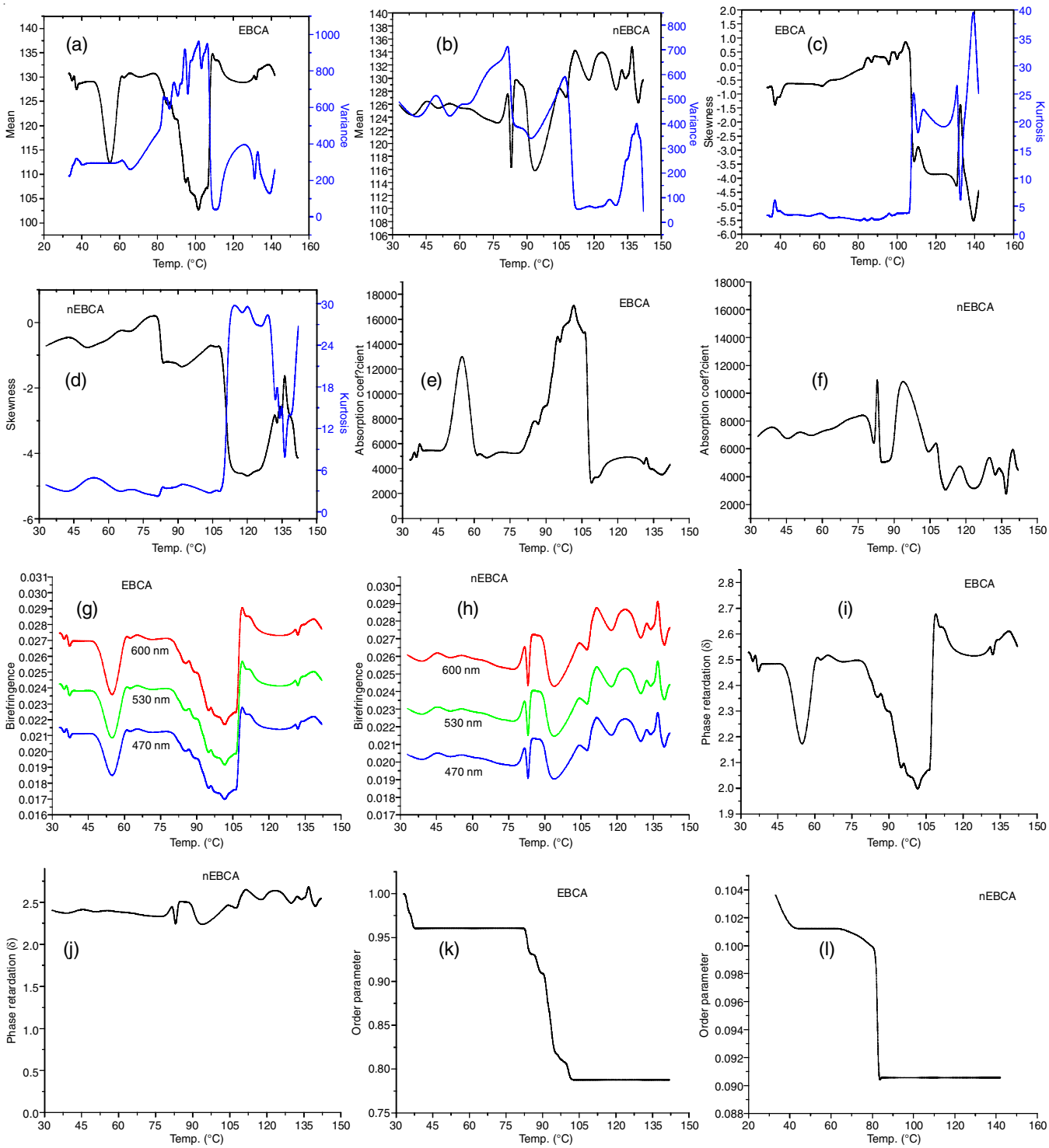

Fig. 8. Image analysis studies of EBCA and ZnO nanoparticles doped EBCA (nEBCA)

TABLE-3
OPTICAL PARAMETERS FOR EBCA & nEBCA

Compound	EBCA	NEBCA
Birefringence	0.029	0.0285
Phase retardation	27	27
Order parameter	0.78	0.090

ºC and then smooth peaks with decreased values of absorption coefficient were observed to isotropic phase.

Birefringence value is maximum (0.029) for both EBCA and nEBCA and was observed at different temperatures 110 and 118 ºC, respectively. The above experimental studies revealed that synthesized ZnO nanoparticles have significant effect on the lattice of EBCA, which means ZnO has developed characteristics of EBCA. The sharp increases, decreases and the fluctuations in the values of computed parameters are due to the changes in the textural features bring variations in the intensity of the image textures. X-Ray diffraction studies of pure (Fig. 9) and ZnO doped EBCA (Fig. 10) also confirm this analysis. Thickness and d-spacing of sample calculated from XRD data are shown in Table-4.

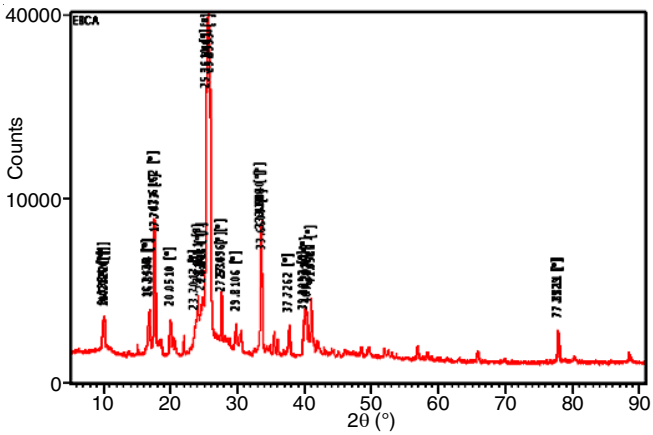

Fig. 9. XRD Pattern of EBCA

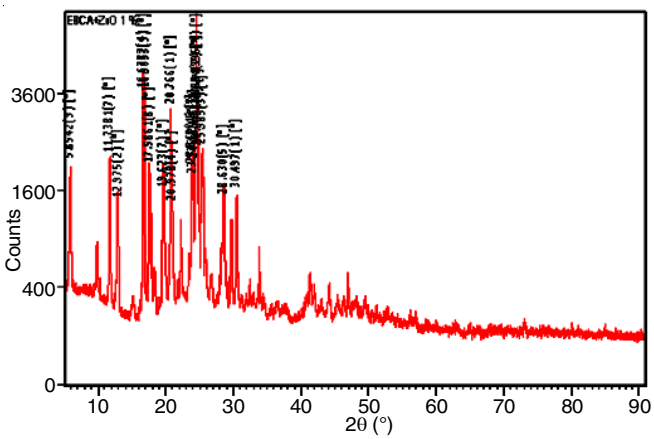

Fig. 10. XRD Pattern of nEBCA

TABLE-4
XRD DATA OF EBCA and nEBCA

Sample	θ_B (°)	FWHM (°)	⟨t⟩ (Å)	d (Å)
EBCA	13.03787	0.1427	619	3.11
nEBCA	3.96534	0.2320	375	3.45

Conclusion

The present study demonstrates that the sensitive image analysis technique with polarizing optical microscopy and identify the phase transition temperatures of nematic liquid crystal *p*-(*p'*-ethoxy benzylidene)-*p*-cyanoaniline (EBCA) and ZnO doped EBCA (nEBCA). It is concluded that each moment of the texture is useful in identifying the transition temperature of EBCA and nEBCA using the stasitical parameters and useful to determine the optical properties. It is observed that transition temperatures (T_{S-N} and T_{N-I}) nano particles dispersed liquid crystal EBCA were increased and this change can be attributed to the presence of ZnO and its interaction with the lattice of EBCA. This in turn help thus to suggest the dispersed nEBCA liquid crystal material as a functional material with vital applications in the field of display technology.

CONFLICT OF INTEREST

The authors declare that there is no conflict of interests regarding the publication of this article.

REFERENCES

1. H. Eskalena, S. Ozgan, U. Alverc and S. Kerl and *Acta Phys. Pol. A*, **127**, 756 (2015); https://doi.org/10.12693/APhysPolA.127.756.
2. S.-T. Wu, U. Efron and L.V.D. Hess, *Appl. Opt.*, **23**, 3911 (1984); https://doi.org/10.1364/AO.23.003911.
3. P. Kohns, J. Schirmer, A.A. Muravski, S.Y. Yakovenko, V. Bezborodov and R. Dąbrowski, *Liq. Cryst.*, **21**, 841 (1996); https://doi.org/10.1080/02678299608032900.
4. T. Akahane, T. Tako and S. Masubuchi, *Opt. Acta Int. J. Opt.*, **26**, 943 (1979); https://doi.org/10.1080/713820098.
5. T.A. El-Dessouki, M. Roushdy, N.I. Hendawy, M.M. Naoum and A.A. Zaki, *J. Mod. Phys.*, **04**, 39 (2013); https://doi.org/10.4236/jmp.2013.41008.
6. S. Chandrasekhar and D. Krishnamurti, *Phys. Lett.*, **23**, 459 (1966); https://doi.org/10.1016/0031-9163(66)91094-8.
7. R. Kandasamy, M. Yamanaka, Y. Izawa and S. Nakai, *Opt. Rev.*, **7**, 149 (2000); https://doi.org/10.1007/s10043-000-0149-z.
8. G. Pelzl and A. Hauser, *Phase Trans.*, **37**, 33 (1991); https://doi.org/10.1080/01411599108203447.
9. T.T. Nguyen, G.-R. Han, C.-H. Jang and H. Ju, *Int. J. Nanomed.*, **10**, 25 (2015); https://doi.org/10.2147/IJN.S88286.
10. R.G. Horn, *J. Phys. (France)*, **39**, 105 (1978); https://doi.org/10.1051/jphys:01978003901010500.
11. K.V.S.N. Raju, S.S. Begum and S. Babu, *J. Pharm. Sci. Res.*, **9**, 269 (2017).
12. G. Si, Y. Zhao, E.S.P. Leong and Y.J. Liu, *Materials*, **7**, 1296 (2014); https://doi.org/10.3390/ma7021296.
13. S.S. Sastry, S.T. Ha, B. Gowri Sankara Rao, K. Mallika and T.V. Kumari, *Liq. Cryst.*, **39**, 1414 (2012); https://doi.org/10.1080/02678292.2012.719041.
14. S.S. Sastry, S. Kumar , T.V. Kumari, K. Mallika, B.G.S. Rao and H.S. Tiong, *Liq. Cryst.*, **39**, 1527 (2012); https://doi.org/10.1080/02678292.2012.725870.
15. A. Tamburini, P. Pitò, A. Cipollina, G. Micale and M. Ciofalo, *J. Membr. Sci.*, **447**, 260 (2013); https://doi.org/10.1016/j.memsci.2013.06.043.
16. B.T.P. Madhav, P. Pardhasaradhi, R.K.N.R. Manepalli, P.V.V. Kishore and V.G.K.M. Pisipati, *Liq. Cryst.*, **42**, 1329 (2015); https://doi.org/10.1080/02678292.2015.1050704.
17. J.P.F. Lagerwall and G. Scalia, *Curr. Appl. Phys.*, **12**, 1387 (2012); https://doi.org/10.1016/j.cap.2012.03.019.

18. G.J. Vroege and H.N.W. Lekkerkerker, *Rep. Prog. Phys.*, **55**, 1241 (1992); https://doi.org/10.1088/0034-4885/55/8/003.
19. C.P. Lapointe, T.G. Mason and I.I. Smalyukh, *Science*, **326**, 1083 (2009); https://doi.org/10.1126/science.1176587.
20. B. In-Su, S.Y. Jeon, S.H. Lee, K.A. Park, S.H. Jeong, K.H. An and Y.H. Lee, *Appl. Phys. Lett.*, **87**, 263110 (2005); https://doi.org/10.1063/1.2158509.
21. I. Haller and I.B.M. Thomas, *Progr. Solid State Chem.*, **10**, 103 (1975); https://doi.org/10.1016/0079-6786(75)90008-4.
22. H. Sackmann and D. Demus, *Mol. Cryst. Liq. Cryst.,* **21**, 239 (1973); https://doi.org/10.1080/15421407308083321.
23. G.R. Luckhurst and C.A. Veracini, The Molecular Dynamics of Liquid Crystals, ASI series: Mathematical and Physical Sciences, vol. 431 (2012).
24. F. Castles, S.M. Morris and H.J. Coles, *AIP Adv.*, **1**, 032120 (2011); https://doi.org/10.1063/1.3624725.
25. R. Van Deun, D. Moors, B. De Fré and K. Binnemans, *J. Mater. Chem.*, **13**, 1520 (2003); https://doi.org/10.1039/B305158G.
26. S. Orlandi, E. Benini, I. Miglioli, D.R. Evans, V. Reshetnyak and C. Zannoni, *Phys. Chem. Chem. Phys.*, **18**, 2428 (2016); https://doi.org/10.1039/C5CP05754J.
27. C.-Y. Tang, S.-M. Huang and W. Lee, *J. Phys. D. Appl. Phys*., **44**, 355102 (2011); https://doi.org/10.1088/0022-3727/44/35/355102.
28. S. Al-Zangana, M. Iliut, M. Turner, A. Vijayaraghavan and I. Dierking, *Adv. Opt. Mater.*, **4**, 1541 (2016); https://doi.org/10.1002/adom.201600351.
29. W.-Z. Chen, Y.-T. Tsai and T.-H. Lin, *Appl. Phys. Lett.*, **94**, 201114 (2009); https://doi.org/10.1063/1.3142390.
30. A. Lorenz, N. Zimmermann, S. Kumar and R. Dean, *Phys. Rev. E.*, **86**, 051704 (2012); https://doi.org/10.1103/PhysRevE.86.051704.
31. W.S. Koo, H.K. Chung, H.G. Park, J.J. Han, H.C. Jeong, M.J. Cho, D.H. Kim and D.S. Seo, *J. Nanosci. Nanotechnol.*, **14**, 8609 (2014); https://doi.org/10.1166/jnn.2014.9953.
32. M. Akimoto, S. Kundu, K. Isomura, I. Hirayama, S. Kobayashi and K. Takatoh, *Mol. Cryst. Liq. Cryst.*, **508**, 363 (2009); https://doi.org/10.1080/15421400903058130.
33. H. Eskalen, S. Özgan, Ü. Alver and S. Kerli, *Acta Phys. Pol.*, **127**, 756 (2015); https://doi.org/10.12693/APhysPolA.127.756.
34. F. Haraguchi, K.-i. Inoue, N. Toshima, S. Kobayashi and K. Takatoh, *Jpn. J. Appl. Phys.*, **46**, L796 (2007); https://doi.org/10.1143/JJAP.46.L796.
35. S.S. Sastry, K. Mallika, T. Vishwam, S. Lakshminarayana and H.S. Tiong, *Liq. Cryst.*, **41**, 558 (2014); https://doi.org/10.1080/02678292.2013.865798.
36. Ch.L. Vineeral, G. Tirumala, S.T. Ha and S.S. Sastry, *Int. J. Eng. Res Appl.*, **7**, 5 (2017); https://doi.org/10.9790/9622-0708030513.
37. R.C. Gonzalez, R.E. Woods and S.L. Eddins, Digital Image Processing Using MATLAB, Dorling Kindersley, Delhi (India), p. 13 (2004).
38. R. Manohar, S.P. Yadav, A.K. Srivastava, A.K. Misra, K.K. Pandey, P.K. Sharma and A.C. Pandey, *Jpn. J. Appl. Phys.*, **48**, 101501 (2009); https://doi.org/10.1143/JJAP.48.101501.